Journal of Thermal Analysis and Calorimetry, Vol. 90 (2007) 1, 67–72

HIGH-TEMPERATURE THERMAL BEHAVIOUR OF Cr-DOPED $LiMn_2O_4$ SPINELS SYNTHESIZED BY THE SUCROSE-AIDED COMBUSTION METHOD

Rosa Maria Rojas[1*], *K. Petrov*[2], *G. Avdeev*[2], *J. M. Amarilla*[1], *L. Pascual*[1] *and J. M. Rojo*[1]

[1]Instituto de Ciencia de Materiales de Madrid, Consejo Superior de Investigaciones Científicas, Cantoblanco, 28049 Madrid, Spain
[2]Institute of General and Inorganic Chemistry, Bulgarian Academy of Sciences, 1113 Sofia, Bulgaria

Chromium doped spinels $LiCr_YMn_{2-Y}O_4$ ($0.2 \leq Y \leq 0.8$) has been synthesized by the sucrose-aided combustion procedure. The thermal behaviour, phase homogeneity and structural characteristics of the samples were studied by thermal analysis, coupled mass spectrometry, and room- and high-temperature X-ray diffraction methods. It was found that the 'as prepared' samples contained residual organic impurities undetectable for X-ray diffraction, that burn out completely at 400°C. Samples treated between 400 and 750°C are single phase spinels, whose crystallites size increase from 10 to 50 nm on increasing the temperature. Cr-doping enhances the thermal stability of the spinels, which augments on increasing the Cr content Y. The enhanced thermal stability of the spinels has been accounted for based on the high excess stabilization energy of Cr^{3+} in octahedral ligand field.

Keywords: *combustion synthesis, high-temperature thermal behaviour, Li–Cr–Mn oxide spinels, lithium batteries, thermal analysis study*

Introduction

Solution combustion synthesis is a novel and competitive method for the synthesis of various types of nano-materials. It is based on an oxidation-reduction reaction between soluble precursor salts (oxidizers) and sacrificial, most often carbonaceous, compounds (fuels). The process is strongly exothermic, self-sustaining and self-propagating. Owing to the release of large volume of thermolysis gaseous products, it results in obtaining a voluminous porous product of loosely packed crystallites [1–8]. Combustion synthesis has many advantages compared to other traditional methods for preparation of finely divided solids: precipitation, thermal decomposition of precursors, sol–gel processes, spray pyrolysis, etc. It is time and energy saving, requires simple equipment and cheap reagents. Most generally, a combustion reaction is controlled by several basic parameters: type of fuel and oxidizer, fuel-to-oxidizer molar ratio, ignition temperature, and relative volume of the evolved gaseous products. The optimal conditions of synthesis using the same fuel depend on the particular composition, and these conditions have to be determined empirically. Recently we have applied this method using metal nitrates as oxidizers and sucrose as fuel, to the synthesis of several undoped, single- and doubly-doped $LiMn_2O_4$-based spinels [9–12]. It has been demonstrated that the spinel products obtained are single-phase compounds and have nanometric particle size.

In this paper we report about the sucrose-aided combustion synthesis of a series of chromium-doped spinels $LiCr_YMn_{2-Y}O_4$ ($0.2 \leq Y \leq 0.8$). They have been characterized by room- and high-temperature X-ray diffraction, thermal analysis and coupled mass spectrometry. Special attention has been paid to their high temperature thermal behaviour and thermal stability.

Experimental

Synthesis of the spinel compounds

Preset stoichiometric amounts of reagent grade $LiNO_3$, $Mn(NO_3)_2{\cdot}4H_2O$ and $Cr(NO_3)_3{\cdot}9H_2O$ were dissolved in a small amount of distilled water. The fuel (sucrose) was then added to the solution, and heated on a hot plate at about 100°C to evaporate the excess water. The liquid adopted a syrupy consistency and gradually transformed to voluminous foam. Raising the temperature up to ≈200°C caused the self-combustion of the reaction body and its transformation to the desired product.

The following formal chemical equation describes the combustion in an adiabatic approximation (closed system), and allows determination of the amount of sucrose, z, needed to obtain 1 mol of the spinel product:

* Author for correspondence: rmrojas@icmm.csic.es

1388–6150/$20.00

Akadémiai Kiadó, Budapest, Hungary
Springer, Dordrecht, The Netherlands

$$LiNO_3 + (2–Y)Mn(NO_3)_2 + YCr(NO_3)_3 +$$
$$+ zC_{12}H_{22}O_{11} = LiCr_YMn_{2–Y}O_4 + 12zCO_2 +$$
$$+ 11zH_2O + (2.5 + 0.5Y)N_2$$

From the oxygen mass balance in the system it follows that:

$$3 + 6(2 – y) + 9y + 11z = 4 + 24z + 11z$$
$$\text{and } z = (11 + 3y)/24$$

It has been found earlier [10–12] that, the combustion is easily controlled when z≈1, and as z depends on Y, the amount of sucrose z was chosen to vary from 0.9 for y=0, to 1.2 for y=1.0.

Instrumental methods

The phase homogeneity and the structural characteristics of the samples were studied by X-ray powder diffraction (XRD). The patterns were recorded at room temperature in a Bruker D8 diffractometer, with CuK_α radiation, in the step scanning mode, at 0.02° (2θ) step and 2 s step^{-1} counting time, within the range 15°≤2θ≤80°. Lattice parameters were refined with the CELREF program [13]. High-temperature XRD patterns were recorded at 1°(2θ) min^{-1} scan rate between 15°≤2θ≤75°, with an Anton Paar chamber mounted on a Philips PW 1710 diffractometer. The powders were mounted onto a Pt/Rh heating strip. The temperature was measured with a Pt–13%Rh/Pt thermocouple. The heating experiments were carried out in still air at temperatures between 25–1100°C, at 2°C min^{-1} heating rate. The temperature was allowed to stabilize for 20 min before each pattern was recorded.

Differential thermal analysis (DTA) and thermogravimetric (TG) curves were simultaneously recorded with a Stanton STA 781 thermal analyzer. Analysis was carried out on the 'as prepared' spinels and on the compounds heated at 750°C for 24 h. The samples were analyzed in the interval room temperature–1100°C in still air atmosphere. The curves were recorded at 10°C min^{-1} heating/cooling rate with Al_2O_3 as inert reference. The mass of the sample used in each run was about 30 mg. The qualitative determination of gases evolved during the thermal treatment was followed with a ThermoStar mass spectrometer (MS) coupled to a DTA/TG Seiko 320 U instrument. Heating and cooling rates were of 10°C min^{-1} and air or argon was used as the gas carrier.

Results and discussion

Samples characterization

The XRD patterns of the 'as prepared' samples (not shown) showed the diffraction peaks of a spinel-type structure, S.G. Fd3m, only. However, to assess the purity of the 'as prepared' samples, we performed a study by DTA/TG/MS of the samples without any previous thermal treatment. Thermal analysis and mass spectrometry curves recorded for all the 'as prepared' samples are similar. As an example, the thermal analysis curves and the mass spectra simultaneously recorded for the 'as prepared' Y=0.2 sample are shown in Fig. 1. Between room temperature and 350°C an exothermic peak and a step are observed in the DTA and TG curves, respectively (Fig. 1a). The mass spectra show signals of CO_2 (m/z=44) and C (m/z=12) with maxima at ≈300°C (Fig. 1b). The exothermic peak and the step can be hence ascribed to the combustion of some organic amorphous impurities [10–12]. These impurities, which are not detectable by X-ray diffraction, indicate that the 'as prepared' samples have some organic residues, which disappear after heating of the samples at 400°C for 1 h. In effect, DTA/TG curves recorded for the samples after the latter thermal treatment do not show either the exothermic effect or the step already mentioned. Between 350 and 400°C the sample undergoes a mass gain that can be related to the specific conditions of the method of synthesis. At the first stages of the reaction, during the swelling process, a local reducing atmosphere is generated due to the thermolysis of the reagents. In these conditions

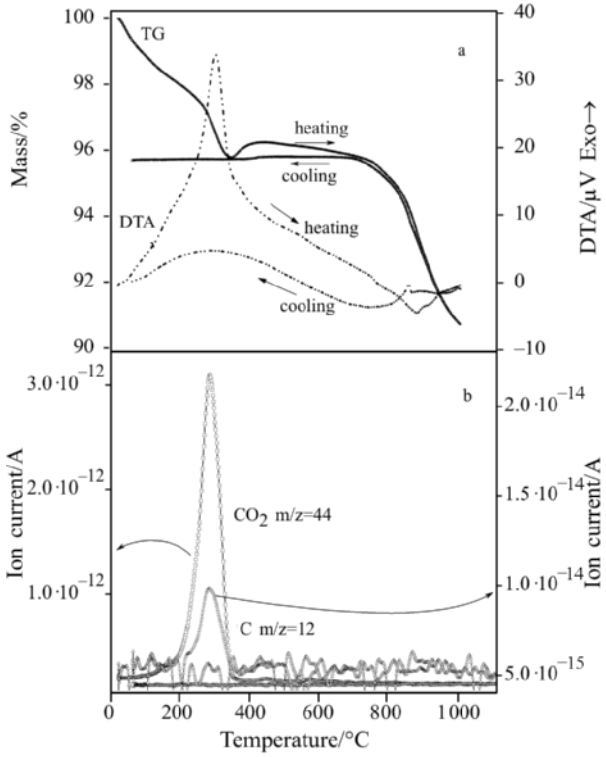

Fig. 1 a – DTA and TG curves of the 'as prepared' $LiCr_YMn_{2–y}O_4$, Y=0.2 spinel; b – mass spectra simultaneously recorded in air flow

some cations could have oxidation states lower than the theoretical ones for spinels. Reduction processes have been also reported for the thermal decomposition of some organic salts [14, 15]. On progressing the heating process an important mass loss is observed above 800°C, which is currently associated with the spinel decomposition [16, 17]. After heating at the maximum temperature (1000°C), the cooling TG curve shows a mass gain between 1000–750°C, and a plateau between 750–20°C. This plateau confirms that the first mass loss on heating occurs in an irreversible way, and support its ascription to removal of organic residues. Moreover, in the high-temperature range, 700–1000°C, the heating DTA curve shows a step-like feature, and a reversible small endothermic peak. These effects will be described in detail in next section.

After heating the as-prepared sample at 400 and 750°C, the samples were cooled to room temperature and XRD patterns were recorded (Fig. 2). All the patterns show lines of spinel-type structure only. The mean crystallite size, calculated from the diffraction line broadening, is about 10 nm for the samples heated at 400°C, and 40 to 50 nm for those heated at 750°C. The variation of lattice parameter, a_c, with composition for the samples heated at 750°C is shown in Fig. 3 (closed symbols). It can be observed that a_c decreases on increasing the Cr-content in the samples. The trend of shrinking of the lattice parameter on increasing Cr-doping has been observed in $LiCr_YMn_{2-Y}O_4$ spinels synthesized by several procedures and at different temperatures [18–21]. The decrease of the lattice parameter has been accounted for by the shrinking of the Mn–O_6 octahedra bond-length, which shortens on increasing the Cr content. This shortening has been ascribed to the following factors: *i*) replacement of Mn^{3+} (ionic radius 0.645 Å) by a trivalent ion Cr^{3+}, having smaller ionic radius, 0.615 Å [22]; *ii*) the higher average oxidation state of Mn on increasing the Cr-doping also reduces the Mn–O bond length, i.e. the unit cell parameter [20]. The linear diminution of a_c on increasing the Cr-doping points to the formation of a solid solution in the whole compositional range. In effect, the a_c values determined for the $LiCr_YMn_{2-Y}O_4$ synthesized in this work range between the reported for the end members of the solid solution, i.e. $LiMn_2O_4$ [35-0782 JCPDS file] and $LiCrMnO_4$ [21].

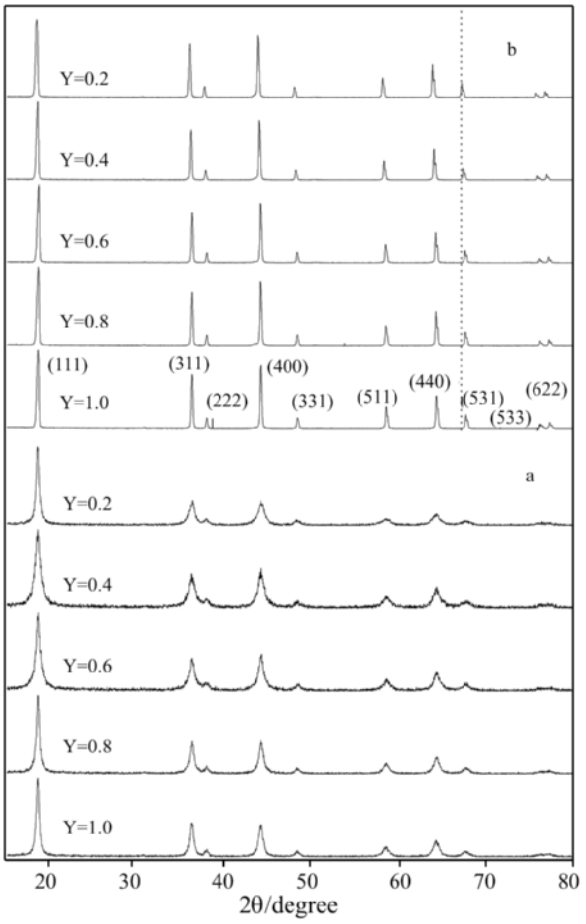

Fig. 2 X-ray diffraction patterns recorded at room temperature for the $LiCr_YMn_{2-Y}O_4$ spinels: a – heated at 400°C for 1 h; b – heated at 750°C for 24 h

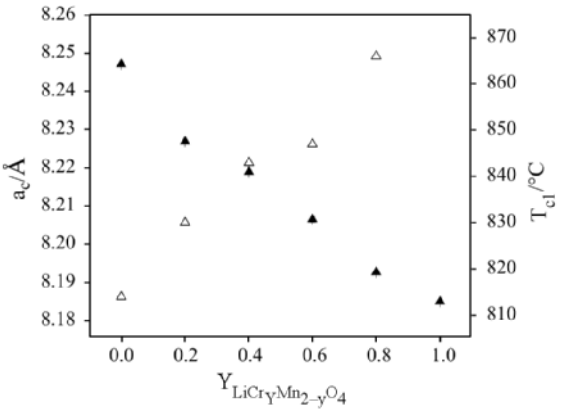

Fig. 3 Plot of the lattice parameter a_c (closed symbols) and of temperature of decomposition T_{c1} (open symbols) of the $LiCr_YMn_{2-Y}O_4$ *vs.* Cr content Y

High-temperature thermal analysis studies

Several studies have been carried out at low temperature on stoichiometric [23, 24], oxygen deficient $LiMn_2O_{4-\delta}$ [25–27], and on M-doped $LiMn_2O_4$ spinels [28–32]. However, high-temperature thermal studies are scarce [29, 30, 33–36] and generally deal with a single composition. Notwithstanding that, high-temperature thermogravimetric analysis has been proposed as a procedure for determining the lithium stoichiometry in $Li_{1+Y}Mn_2O_4$ spinels [37]. We have

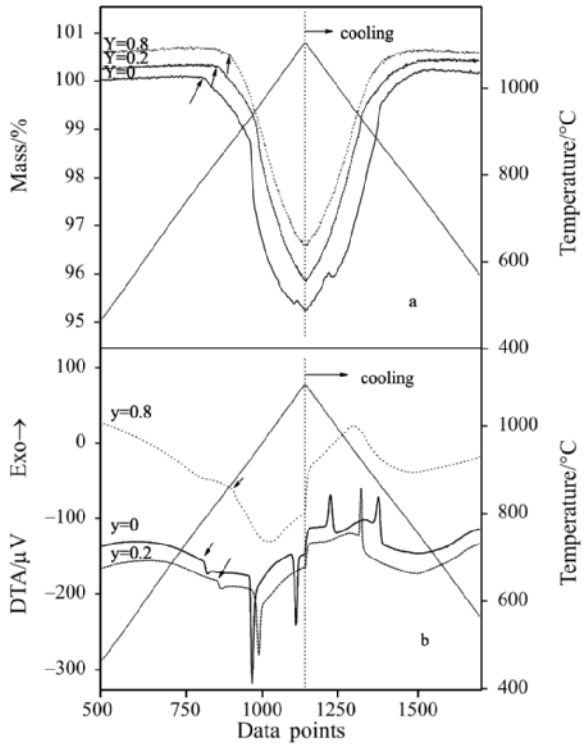

Fig. 4 Thermal analysis curves of the 750°C-heated $LiCr_YMn_{2-Y}O_4$ spinels: a – TG curves (for sake of clarity TG curves have been shifted); b – DTA curves. Only the high-temperature region is shown

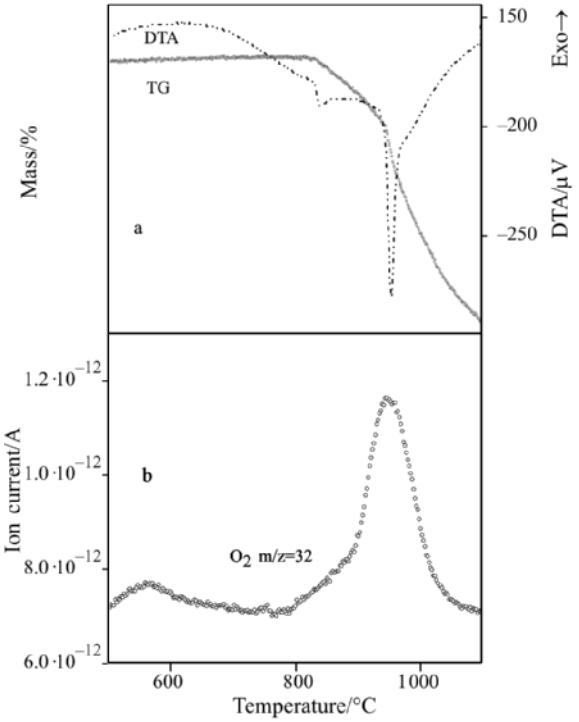

Fig. 5 a – DTA/TG curves of the 750°C-heated $LiCr_{0.2}Mn_{1.8}O_4$ spinel; b – mass spectrum simultaneously recorded in argon flow

considered worthwhile to assess if variations in the Cr-content are also revealed in the high-temperature thermal behavior of the $LiCr_YMn_{2-Y}O_4$ spinels. In Fig. 4 TG/DTA curves recorded for 750°C-heated $LiCr_{0.2}Mn_{1.8}O_4$ and $LiCr_{0.8}Mn_{1.2}O_4$ spinels are shown. Curves recorded for $LiMn_2O_4$ have also been included for comparison. Only the high-temperature region is depicted in the figure, and no thermal effects are observed below 700°C. The curves show some common features; particularly the thermogravimetric ones (Fig. 4a). They indicate that the spinels remain stable up to ≈800°C. From this temperature a change in the slope of the TG curves, which is more evident for the low-doped samples, is observed. The onset temperature of this first step, (T_{C1}, arrow marked in Fig. 4a) ranges in a wide region from ≈828°C for the sample at Y=0.2 to ≈865°C for the sample at Y=0.8. On increasing the temperature and between the T_{C1} and 1100°C, the spinels undergo a very pronounced mass loss with associated endothermic effects, as shown the DTA curves (Fig. 4b). The coupled DTA/TG/ mass spectrum (Fig. 5) recorded in argon atmosphere for the $LiCr_{0.2}Mn_{1.8}O_4$ spinel up to 1100°C shows, simultaneously to the mass loss observed in the TG curve (Fig. 5a), a signal of O_2 (m/z=32) with maximum at ≈950°C (Fig. 5b), which indicates that the pronounced mass loss is due to oxygen removal. TG curves recorded on cooling (Fig. 4a) show that for the $0 \le Y \le 0.8$ spinels, the mass loss on heating is regained on cooling. Consequently the observed mass losses observed at T>800°C are ascribed to the evolution of oxygen, which is almost totally regained on cooling to room temperature. The DTA curves (Fig. 4b) show step-like features (arrow marked in the figure) at the same temperatures of the first change in slope in the TG curves, though their sharpness is worse defined as the dopant content increases. The endothermic effects observed in the DTA curves of the samples at Y=0 and 0.2, with peak temperature of ≈920°C, are associated with the very pronounced mass loss undergone by the samples between ≈850 and 1100°C. These endothermic peaks broadens on increasing the amount of Cr-dopant, and for the sample at Y=0.8 it is very broad and poorly defined. It is worth to mention that the second strong endothermic peak recorded in the DTA curve of $LiMn_2O_4$ at ≈1057°C has disappeared for the samples with $Y \ge 0.2$. In the cooling DTA curves we observe the presence of exothermic peaks between 1100 and 800°C, which coincides with the mass gains recorded in the cooling TG curves. It follows that we are dealing with reversible oxygen removal/uptake processes. Moreover, the XRD patterns recorded on the residues of thermal analysis up to 1100°C (not shown) are similar to those of the starting spinels, the only difference consists in the narrowing of the diffraction peaks.

The value of T_{C1} *vs.* composition determined from the respective DTA curves of the $LiCr_YMn_{2-Y}O_4$ spinels has been plotted in Fig. 3 (open symbols). The T_{C1} temperature has been considered to represent the upper stability line of the spinels [17], and as it has been indicated before, at this temperature oxygen removal from the spinel structure has been demonstrated. So, T_{C1} can be considered as the temperature limit at which the spinel is stable. In the case of the Cr-doped spinels Yamaguchi *et al*. have pointed out that the standard enthalpy of formation for the Cr-doped spinels decreases on increasing the Cr-content [33]. Their values range between –1411.6 kJ mol^{-1} for the spinel at Y=0.083 to –1430.7 kJ mol^{-1} for the compound at Y=0.333. This decrease in the enthalpy of formation of Cr-doped spinels, which is opposite to the one shown by the Co- and Ni-doped spinels [33], agrees with the observed almost linear increase observed in the T_{C1} on increasing the Cr-doping (Fig. 3, open symbols). The enhancement of thermal stability of Cr-doped spinels can be accounted for bearing in mind that Cr^{3+} is, together with Mn^{3+}, the ion with the greatest excess octahedral stabilization energy. For Cr^{3+} the estimated octahedral stabilization energy is 224.83 kJ mol^{-1}, and for Mn^{3+} it is 135.65 kJ mol^{-1} [38]. Hence it is likely to assume that the progressive substitution of Mn^{3+} by Cr^{3+} in octahedral sites, results in stabilization of the spinel structure and consequently, the T_{C1} temperature increases on Cr-doping.

High-temperature X-ray diffraction studies

To elucidate the phase transformations associated with the thermal treatment, high-temperature XRD measurements were carried out on the $LiCr_{0.2}Mn_{1.8}O_4$ and $LiCr_{0.8}Mn_{1.2}O_4$ samples. The two spinels followed clearly different pathways on heating, and Fig. 6 shows some of the patterns recorded for these two samples. It can be seen that the pattern of the $LiCr_{0.2}Mn_{1.8}O_4$ spinel at 950°C, (Fig. 6b) shows, in addition to the diffraction peaks of the spinel, another low intensity peaks of Li_2MnO_3 [cross marked in Fig. 6b; 84-1634 JCPDS file]. On the contrary, the pattern recorded at 950°C for the $LiCr_{0.8}Mn_{1.2}O_4$ spinel (Fig. 6d) shows that the compound remains stable. The pattern does not modify, and only some broadening of the peaks is observed. However, at this temperature, and according to TG results, the spinel has undergone a mass loss of about 1.4%. This result seems to indicate that the highly Cr-doped $LiCr_{0.8}Mn_{1.2}O_4$ spinel is very stable to heat treatments and, that albeit the oxygen removal undergone up to 950°C, the highly Cr-doped $LiCr_{0.8}Mn_{1.2}O_4$ spinel

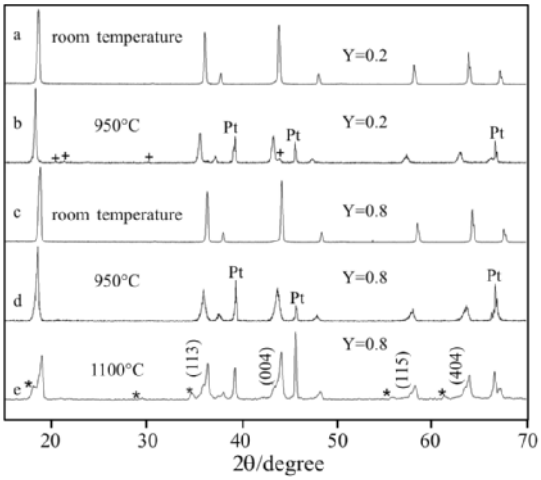

Fig. 6 X-ray diffraction patterns of $LiCr_{0.2}Mn_{1.8}O_4$ and $LiCr_{0.8}Mn_{1.2}O_4$ recorded at the temperatures indicated. (+ – Li_2MnO_3; * – $MnCr_2O_4$; indexing corresponds to the tetragonal $I4_1/amd$ spinel phase; Pt lines are from the sample holder.)

neither decomposes nor transforms into the tetragonal $I4_1/amd$ phase reported for the oxygen-deficient $LMn_2O_{4-\delta}$ spinels formed at high temperature [16, 36]. The latter result can be accounted for having in mind that in the Y=0.8 spinel the amount of the Jahn–Teller cation Mn^{3+} is very low and hence, distortion is not as favoured as it is in $LiMn_2O_4$ spinel. However, in the pattern recorded at 1100°C (Fig. 6e) a tetragonal spinel with lattice parameter a_T=8.22 Å, c_T=8.30 Å can be identified. Moreover, some other peaks of low intensity, which can be tentatively ascribed to chromium manganese spinel $MnCr_2O_4$ (star marked in Fig. 6d; 75-1614 JCPDS file) are also observed. At 1100°C, the mass loss undergone by the $LiCr_{0.8}Mn_{1.2}O_4$ spinel is ≈4% of the initial mass. These results may well suggest that the $LiCr_{0.8}Mn_{1.2}O_4$ spinel decomposes in a mixture of tetragonal $LiMn_2O_{4-\delta}$ and $MnCr_2O_4$, according to the reaction:

$$5/2LiCr_{0.8}Mn_{1.2}O_4 \rightarrow LiMn_2O_{4-\delta} + MnCr_2O_4 + \\ + 3/4Li_2O + \delta/2O_2$$

On cooling the sample to room temperature in the high-temperature XRD chamber, the pattern recorded at room temperature is not very much different from the one recorded at 1100°C. However, the pattern recorded at room temperature on the residue of thermal analysis of the $LiCr_{0.8}Mn_{1.2}O_4$ sample was similar to that of the starting compound. It might be accounted for by the very different experimental conditions of the high-temperature XRD and of the thermal analysis experiments. In the former, the heating process is slow, the temperature is allowed to stabilize for some minutes, and the recording time is ≈1 h. This prolonged

heating in the high-temperature XRD chamber can result in the formation of $LiMn_2O_{4-\delta}$ and $MnCr_2O_4$ compounds that are not re-oxidized on a very fast cooling. In the thermal analysis, carried out up to 1100°C, the samples are dynamically heated/cooled at 10°C min^{-1}. At these conditions they can recover on cooling, almost 100% of the mass loss on heating.

Conclusions

The sucrose-aided combustion synthesis is a promising tool for preparation of Cr-doped lithium manganese oxide spinels, having small particle size. Due to the high excess octahedral stabilization energy of Cr^{3+}, the Cr-doped $LiMn_2O_4$ spinels show thermal stability higher than the undoped $LiMn_2O_4$, and it increases on increasing the dopant content. The thermal behaviour of the Cr-doped spinels varies with the amount of chromium. This behaviour has been followed by using thermo-analytical tools in combination with high-temperature XRD methods.

Acknowledgements

Financial support through the projects MAT 2005-01606 (MEC), GR/MAT/0426/2004 (CAM) and the joint project CSIC-Bulgarian Academy of Sciences no. 2004BG0010 is thankfully recognized.

References

1 J. J. Kingsley and K. C. Patil, Mater. Lett., 6 (1988) 427.
2 H. C. Yi and J. J. Moore, J. Mater. Sci., 25 (1990) 1159.
3 S. S. Manoharan, N. R. S. Kumar and K. C. Patil, Mater. Res. Bull., 25 (1990) 731.
4 Y. Zhang and G. C. Stangle, J. Mater. Res., 9 (1994) 1997.
5 D. Huang, K. R. Venkatachari and G. S. Stangle, J. Mater. Res., 10 (1995) 762.
6 E. J. Bosze, J. McKittrick, G. A. Hirata and L. E. Shea, C. R. Ronda, K. S. Misra, L. Shea, A. Srivastava and H. Yamamoto, Eds, Physics and Chemistry of Luminescent Materials, 99-40, Honolulu, Hawaii, 1999, Electrochem. Soc. Symp., Proc., p. 176. 7 T. Mimani and K. C. Patil, Mater. Phys. Mech., 4 (2001) 134.
8 R. Garcia, G. A. Hirata and J. McKittrick, J. Mater. Res., 16 (2001) 1059.
9 D. Kovacheva, H. Gadjov, K. Petrov, S. Mandal, M. G. Lazarraga, L. Pascual, J. M. Amarilla, R. M. Rojas, P. Herrero and J. M. Rojo, J. Mater. Chem., 12 (2002) 1184.
10 M. G. Lazarraga, L. Pascual, H. Gadjov, D. Kovacheva, K. Petrov, J. M. Amarilla, R. M. Rojas, M. A. Martín-Luengo and J. M. Rojo, J. Mater. Chem., 14 (2004) 1640.
11 L. Pascual, H. Gadjov, D. Kovacheva, K. Petrov, J. M. Amarilla, P. Herrero, R. M. Rojas and J. M. Rojo, J. Electrochem. Soc., 152 (2005) A301.
12 R. M. Rojas, J. M. Amarilla, L. Pascual, J. M. Rojo, D. Kovacheva and K. Petrov, J. Power Sources, 160 (2006) 529.
13 J. Laugier and A. Filhol, CelRef, PC version (unpublished) ILL, Grenoble, France (1991).
14 M. D. Judd, B. A. Plunkett and M. I. Pope, J. Thermal Anal., 6 (1974) 555.
15 L. Patron, O. Carp, I. Mindru, G. Marinescu and E. Segal, J. Therm. Anal. Cal., 72 (2003) 281.
16 M. M. Thackeray, M. F. Mansueto, D. W. Dees and D. R. Vissers, Mater. Res. Bull., 31 (1996) 133.
17 J. M. Paulsen and J. R. Dahn, Chem. Mater., 11 (1999) 3065.
18 W. Baochen, X. Yongyao, F. Li and Z. Dongjiang, J. Power Sources, 43 (1993) 539.
19 C. Sigala, D. Guyomard, A. Verbaere, Y. Piffard and M. Tournoux, Solid State Ionics, 81 (1995) 167.
20 S.-J. Hong, S.-H. Chang and Ch.-H. Yo, Bull. Korean Chem. Soc., 20 (1999) 53.
21 M. Kaneko, S. Matsuno, T. Miki, M. Nakayama, H. Ikuta, Y. Uchimoto, M. Wakihara and K. Kawamura, J. Phys. Chem. B, 107 (2003) 1727.
22 R. D. Shannon, Acta Crystallogr., A32 (1976) 751.
23 A. Yamada and M. Tanaka, Mater. Res. Bull., 30 (1995) 715.
24 G. Rousse, C. Masquelier, J. Rodríguez-Carvajal and M. Hervieu, Electrochim. Solid State Lett., 2 (1999) 6.
25 J. Sugiyama, T. Atsumi, A. Koiwai, T. Saski, T. Hioki, S. Noda and N. Kamegashira, J. Phys. Condens. Matter., 9 (1997) 1729.
26 Y. Xia, T. Sakai, T. Fujieda, X. Q. Yang, X. Sun, Z. F. Ma, J. Mc Breen and M. Yoshio, J. Electrochem. Soc., 148 (2001) A723.
27 M. Tachibana, T. Tojo, H. Kawaji and T. Atake, Phys. Rev., B68 (2003) 094421.
28 G. G. Amatucci, C. N. Schmutz, A. Blyr, C. Sigala, A. S. Godz, D. Larcher and J. M. Tarascon, J. Power Sources, 69 (1997) 11.
29 T. Tsuji, M. Nago, Y. Yamamura and N. Tien Tai, Solid State Ionics, 154 (2002) 381.
30 R. Dziembaj and M. Molenda, J. Power Sources, 119-121 (2003) 121.
31 H. Ikuta, K. Tanaka and M. Wakihara, Thermochim. Acta, 414 (2004) 227.
32 J. Molenda, D. Pałubiak and J. Marzec, J. Power Sources, 144 (2005) 176.
33 R. Yamaguchi, H. Ikuta and M. Wakihara, J. Therm Anal. Cal., 57 (1999) 797.
34 J. M. Tarascon, W. R. McKinnon, F. Coowar, T. N. Bowmer, G. Amatucci and D. Guyomard, J. Electrochem. Soc., 141 (1994) 1421.
35 Z. Wang, H. Ikuta, Y. Uchimoto and M. Wakihara, J. Electrochem. Soc., 150 (2003) A1250.
36 A. Yamada, K. Miura, K. Hinokuma and M. Tanaka, J. Electrochem. Soc., 142 (1995) 2149.
37 Y. Gao and J. R. Dahn, Appl. Phys. Lett., 66 (1995) 2487.
38 D. Dunitz and L. E. Orgel, Advances in Inorganic Chemistry, Academic Press Inc., San Diego 1960, Vol. 2, pp. 1–60.

DOI: 10.1007/s10973-007-8477-x